lubricants

MDPI

Article

CPU Performance Improvement Using Novel Thermally Conductive Carbon Nano Grease

Travis Grablander [1], Greg Christensen [1,*], Craig Bailey [1], Ding Lou [2], Haiping Hong [2] and Hammad Younes [2,*]

[1] Novum Nano, Rapid City, SD 57701, USA; travis.grablander@novumnano.com (T.G.); craig.bailey@novumnano.com (C.B.)
[2] Department of Electrical Engineering, South Dakota School of Mines and Technology, Rapid City, SD 57701, USA; ding.lou@mines.sdsmt.edu (D.L.); haiping.hong@sdsmt.edu (H.H.)
* Correspondence: greg.christensen@novumnano.com (G.C.); hammad.younes@sdsmt.edu (H.Y.)

Abstract: Electronics depend on their ability to shed operational heat to maintain operating temperature. Inferior grease can create preventable problems in electronics. This is typically achieved through a thermal grease or paste. If this grease fails to dissipate heat or maintain thermal contact, then the equipment will have faults. Greases with less-than-optimal performance create excessive wear, heat, and reduced life expectancy. This can cause equipment failures and malfunctions at the most inopportune moments. Thermal greases are applied to Central Processors (CPU) and Graphics Processors (GPU) in avionics LRUs, computers, Solar panels, HVAC systems, and other electronics. A high-performance novel nano grease will shed excess heat and increase device life expectancy. The fabricated nano greases show improvements of up to 80% in thermal conductivity measurements. CPU testing resulted in a 100% decrease in the standard deviation of temperature variation from commercial greases.

Keywords: carbon nano grease; hydrogen bonding; thermal conductivity; boron nitride

check for updates

Citation: Grablander, T.; Christensen, G.; Bailey, C.; Lou, D.; Hong, H.; Younes, H. CPU Performance Improvement Using Novel Thermally Conductive Carbon Nano Grease. *Lubricants* **2022**, *10*, 172. https://doi.org/10.3390/lubricants10080172

Received: 11 June 2022
Accepted: 22 July 2022
Published: 27 July 2022

1. Introduction

As the technology matures and computer chips grow smaller in areas such as electronics, communications, aerospace, transportation, and manufacturing, the need for high-performance heat-transfer materials has arisen [1–3]. In many cases, higher performance means more heat, which becomes a limiting factor in electronics design. The reliability of devices exponentially relies on their operating temperature [3,4]. Hence, a slight change in the device's operating temperature can lead to a two-times decrease in its lifetime. To maintain the device temperature within the accepted heat levels, generated heat should be removed as quickly as possible. Generally, the generated heat is dissipated using heat sinks [5,6].

However, interfacial thermal resistance, because of the mismatch resulting from the surface roughness of the device and the heat sink's non-surface flatness, decreases the heat-dissipation efficiency of the heat sinks. Therefore, to solve the interfacial thermal resistance, a novel and smooth texture material should be developed and used to solve the heat-dissipation problem. The new material should have properties such as low–medium viscosity, high thermal conductivity, fit with the surface topography of the device surfaces, and ability to take the place of air by filling in the gaps at the interface. Air has a very poor thermal conductivity, 0.02587 W/mK at 20 °C [7]. Air pockets cause heat to stay significantly longer in the CPU case, which in normal cases causes performance drops through thermal throttling or, in rare cases, a melted CPU.

One main approach to solve the air spaces is by utilizing thermal paste. Recently, Shishkin's group comprehensively investigated the thermal conductivities of silicone-oil-based greases and their heat-dissipation performance when applied to a CPU bench [8]. Computer applications and their associated processing demands can vary greatly. In research and other fields, simulation is a powerful tool for testing and requires heavy computation power and memory usage. E-sports is a constantly growing video-game competition market. Leading-edge greases and pastes allow PC enthusiasts to overclock their hardware for significantly improved performance. However, this does come with the tradeoff of potentially causing fatal crashes or overheated systems. Many materials can be used to make a thermal paste/grease. Examples range from liquid metal, a costly yet almost-perfect solution, to toothpaste. Nanomaterials such as CNTs and hBN have great potential in adding to this market with their superior thermal properties. The remarkable mechanical properties and the high thermal conductivity of carbon nanomaterials at a low-weight percentage have opened opportunities in many applications such as CNTs nanogrease [9]. Wu et al. used 20 wt% a few-layer graphite to fabricate thermal-interface materials. By adding 2.5–7.5 wt% of Cu particles. The thermal conductivity improved of 20 wt% of a few-layer graphite and 7.5 wt%. Cu particles with polydimethylsiloxane had a thermal conductivity of 5.96 W/mK through the plane and 41.7 W/mK in plane [10]. Li reported on a fabricated thermal-interface materials from polybutadiene and graphite that had a through plane thermal conductivity of 64.90 W/mK [11].

Chen et al. studied the enhanced dispersion and highly efficient heat-transfer paths of functionalized CNTs in silicone grease as thermal-interface materials [12]. Boron nitride (BN) has been widely reported as an ideal filler for thermal grease due to its high thermal conductivity, low density, and electrically insulating properties [13]. Ge et al. reported significantly improved heat-transfer performance of the cooling system using silicon oil/BN grease [14]. Comprised in the grease are both multi-wall CNTs and hBN in varying proportions. Christensen et al. [15] reported that glycerol fluid increases by >50%, and silicon oil has an increase of 86%. For hBN, Christensen et al. [16] showed that using hBN can enhance both the thermal conductivity and lubricity of the base oils in addition to CNTs. However, BN-based thermal greases often require a higher loading percentage of BN due to their particle shape and low compatibility with the base oil. One solution to increase thermal conductivity with lower filler fractions is to use hybrid fillers with different dimensions and sizes. Hybrid fillers have been reported to have synergistic effects that form 3D percolation structures for improved heat transportation [17–19]. Liang et al. studied reduced graphene oxide (RGO)/hBN hybrid fillers as nano additives to silicone thermal grease. Due to the 3D structure of the stacking of heterostructure RGO and hBN, the fabricated nanogrease exhibited higher thermal conductivity and improved thermal-management performance, compared to silicone grease containing only hBN [20].

Younes et al. discuss the effect of using carbon nanotubes in the thermal and electrical conductivity of grease. It was found that some carbon nanomaterials can make stable and homogenous grease. However, other carbon nanomaterials cannot make stable and homogenous grease. This stability and homogeneity of the fabricated grease was ascribed to the formation of the 3D network formation that the carbon nanomaterials can make. Moreover, the fabricated CNTs grease had a high thermal conductivity [11,21]. Christensen et al. also examined the impact of using carbon nanofibers in the thermal and electrical conductivity of grease. The study found that the thermal conductivity improved by 163.3% when only 5 wt% of carbon nanofibers were used to fabricate the NYE 758G grease. However, 1.4 wt% of MWNT-OH in Krytox XHT750 oil had a thermal conductivity of 37.8% improvement. Grease made of Petro-Canada N650HT oil with 7.5 wt% MWNT-OH had a resistivity of 22.4 Ω cm, whereas the thermal conductivity of similar sample made from MYNTs had resistivity of 7880 Ω cm. this improvement in thermal conductivity is attributed to the hydrogen bonding created between the oil and the MWNT-OH. This assumption was supported by the lowest resistivity results (10.0 Ω cm) that obtained for mixing two solutions capable of making hydrogen bonding (75% glycerol and 25% water) with 4.5 wt% MWNT-OH) [15,22].

Nazari et al. compared the CPU cooling performance of CNT nanofluids with plain ethylene glycol and obtained a 4% difference in convective heat transfer coefficient [23]. Another research by Ebrahimi et al. numerically evaluated the cooling performance of

CNT nanofluid in a microchannel heat sink (MCHS). It was reported that the temperature gradient of the MCHS decreased as the increase of the thickness of CNT-water nanolayer. In addition, the authors found that the thermal resistance of the MHS with cylindrical CNT nanofluid was much lower compared to nanofluid that contains spherical nanoparticles [24]. Guo et al. applied a dynamic model and studied the heat transfer coefficient (HTC) of zinc oxide/water nanofluid in a microfin heat sink. At a volume concentration of 3% zinc oxide in water, the HTC of the dynamic model enhanced by 38.3%. It was concluded that the heat transfer efficiency of the nanofluid increased with higher concentration of nanoparticles and lower particle sizes [25].

The fabricated thermal greases are applied to Central Processors (CPU) and Graphics Processors (GPU) in avionics LRUs, computers, and solar panels, HVAC systems, and other electronics. A high-performance novel nano grease will shed excess heat and increase device life expectancy.

In this work, two types of silicone oil were used to produce our greases, labeled as Phenyl Methyl Silicone (PMS) oil and Polydimethylsiloxane (PDMS). The structures of both oils contain oxygen atoms outside functional groups, which suggests that they will form hydrogen bonds with our CNTs. Although thermal-conductivity performance greatly increases from the addition of functionalized nanotubes, electrical conductivity will also increase [22]. The electrically conductive material can damage sensitive electronics, if it leaks off the CPU and contacts other components. Since silicone oils are dielectric in nature, and hBN is an excellent electric insulator, electrical conductivity is not a major problem. Grease was fabricated by following the method from [26], where a Ross three-roll-milling machine used to fabricate CNT-grease (Figure 1A) was used to disperse the CNTs in the oil, a Hot DiskTM thermal-constants analyzer (Figure 1B) was used to measure the thermal conductivity, and a custom 1 cm^3 cube was 3D-printed specifically for grease measurements through the four-point probe setup (Figure 1C,D). The greases are milled to increase dispersion throughout the sample. A grease made with a higher concentration of CNTs will result in a sticky and flaky substance, whereas higher hBN concentrations will keep the oil as a fluid. The flash points of fabricated greases are around 277 °C.

Figure 1. (**A**) Ross three-roll-milling machine used to fabricate CNT grease. (**B**) Hot DiskTM thermal-constants analyzer. (**C**) A custom 1-cm cube is 3D-printed specifically for grease measurements. (**D**) The four-probe setup for electrical conductivity measurement.

This paper shows that our effort resulted in extremely promising thermally conductive grease/paste with high electrical-insulating properties, so completing this development will provide the market with a more reliable and higher performing grease for electronics. In contrast to traditional and nonconductive commercially available grease, the thermally conductive grease/paste has a high thermal conductivity at a very low weight-percentage loading of the CNTs. In addition, the thermally conductive grease/paste is stable at high temperatures. To improve the grease's thermal conductivity, new base oils capable of hydrogen bonding with the hydroxyl functionalized CNTs (CNTs-OH) will be used. The hydrogen bonding creates a pathway that improves the thermal conductivity of the bulk material. Normally it is very difficult to take advantage of the superior properties of individual carbon nanotubes, as the junctions/gap between the tubes is often so large that it creates a barrier, which defeats the many advantages of carbon nanotubes. Adding functional groups such as hydroxyl groups can bridge this gap between tubes and overcome it. This also allows for bonding with the solvents and base fluids.

2. Materials and Methods

Industrial-grade multiwalled carbon nanotubes functionalized with hydroxyl groups (MWNT-OH), with 20–40 nm diameter, 10–30 µm length, and 95% purity, were purchased from Nanostructured & Amorphous Materials, Inc. 16840 Clay Rd # 113, Houston, TX 77084, USA. Hexagonal boron nitride with an average size of 70 nm was purchased from Lower Friction (M.K. Impex Corp., 6382 Lisgar Dr Mississauga, ON L5N 6X1, Canada). Phenyl methyl silicone oil (PMS) was purchased from Amazon. PMS base oil and nanomaterials were mixed and milled repeatedly using a three-roll mill (Ross Engineering Inc., New York, NY, USA) until stable and homogeneous grease samples were obtained. Scanning electron microscope (SEM) images were obtained using a Zeiss™ Supra40 variable-pressure field-emission SEM). TEM images were taken by JEOL JEM-2100 LaB6 transmission electron microscope (TEM). The computer testing is done on a test bench equipped with an EVGA X299 micro ATX motherboard and an Intel Core I9 7900X CPU and cooled with a Noctua DH-15 air cooler. Prime 95 was selected for thermal-performance testing.

3. Results

CNTs were used to fabricate the thermal grease used in this study, and the TEM and SEM images in Figure 2A,B show that the CNTs are MWNTs. Figure 1C shows the SEM for the hexagonal boron nitride. The fabricated grease from the MWNTs, hBN, and oil is homogenous and stable, as shown in Figure 2D. Prime 95 was selected for thermal-performance testing. This software is primarily used to find prime numbers through FFT calculations, but PC enthusiasts use its stress-test capability to determine the stability of their systems when overclocking.

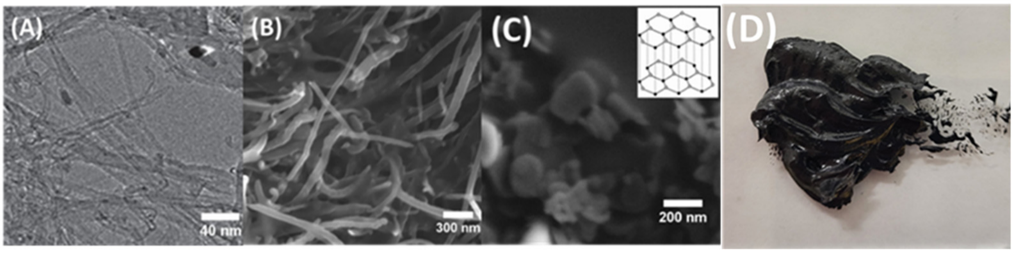

Figure 2. (**A**) TEM image for pristine CNTs used to fabricate the CNTs grease. (**B**) SEM image for the fabricated CNT grease. (**C**) SEM for the hexagonal boron nitride. The inset picture shows the chemical structure of hBN and (**D**) a picture of the fabricated grease.

We set the software to run FFTs of a selected size of 8k by 8k, the lowest size FFT for customization, which stresses the CPU primarily and not the RAM. A stress test set this way loads the entirety of the CPU through floating-point calculations. Since the CPU is under a 100% load throughout the stress test, a large amount of heat is generated [27]. A hardware monitor is used for logging data into CSV files from the motherboard, which are then extracted into the origin lab for quick calculations. Data are logged every half second, with each test running for one hour.

Our stress tests were done at two specific frequencies, the first at regular operation at 3.3 GHz, and the second overclocked at 3.9 GHz. The overclock frequency is much less than the maximum because when using Kryonaut, speeds above 3.9 GHz caused drastic performance changes throughout the 1-h testing period. Thus, 3.9 was chosen due to the stability of the processor under 100% load over the entire hour [27]. For each test, there will be a significant drop in processor speed compared to its set point, and this is due to the load of the CPU and the motherboard trying to compensate for the consistent increased power demand.

Data from almost every major component of the computer are logged, but the primary focus is on the 10 cores of the processor. Three areas of data were selected from the data logs: the first is power consumption, the second is core temperatures, and the third is core clock speeds. Package power is a representative of how hard the CPU is working. CPU core temperatures will determine how well the thermal compound can conduct heat from the CPU shield to the heat sink. Clock speeds are dependent on how hot the current package temperature is and will, consequently, affect power consumption. Each of these three factors should be analyzed as concurrently as possible to determine a reliable thermal compound.

Focusing on the 3.3 GHz tests in Figure 3, we see that only one sample had a significant dip in power consumption. The difference between PMS 3-15 and Kryonaut is roughly 8.85%. It also had the lowest standard deviation of the entire group, making it the most stable-performing compound for this type of test. Figure 4 also shows that this paste was the second-coolest compound out of this group. Kryonaut had a mean temperature of 60 °C, and PMS 3-15 had a mean of 62.5 °C. Figure 5 shows the core average clock speed for this group. For this test speed, the data here are not too significant, other than the stability of PMS 3-15.

Looking at the 3.9 GHz tests in Figure 3, MX4 had a much lower average power consumption than any other compound. Its standard deviation was higher than both of our thermal greases, although 0.9 for an SD value is still very good. PMS 3-15 had a lower consumption than Kryonaut, similar to the previous speed tests. It should be clarified that a lower power is not always a good sign; as stated before, a higher power consumption typically infers a full-throttle CPU. This can be further elaborated on by looking at both Figures 4 and 5.

In Figure 4, MX4 had the second-coolest core temperature average. However, we can see the real reason behind this in Figure 5. This compound's average core clock speed was 3235.6 MHz, which is significantly lower than all other compounds at this operation. This drop-in clock speed is the source of the power drop and lower temperature.

PMS 3-15 again proved to be the most stable compound of the group, with a 5.5 standard deviation for clock speed. The average clock speed is only slightly lower than Kryonaut, and the average core temperature is only 5 °C higher than Kryonaut.

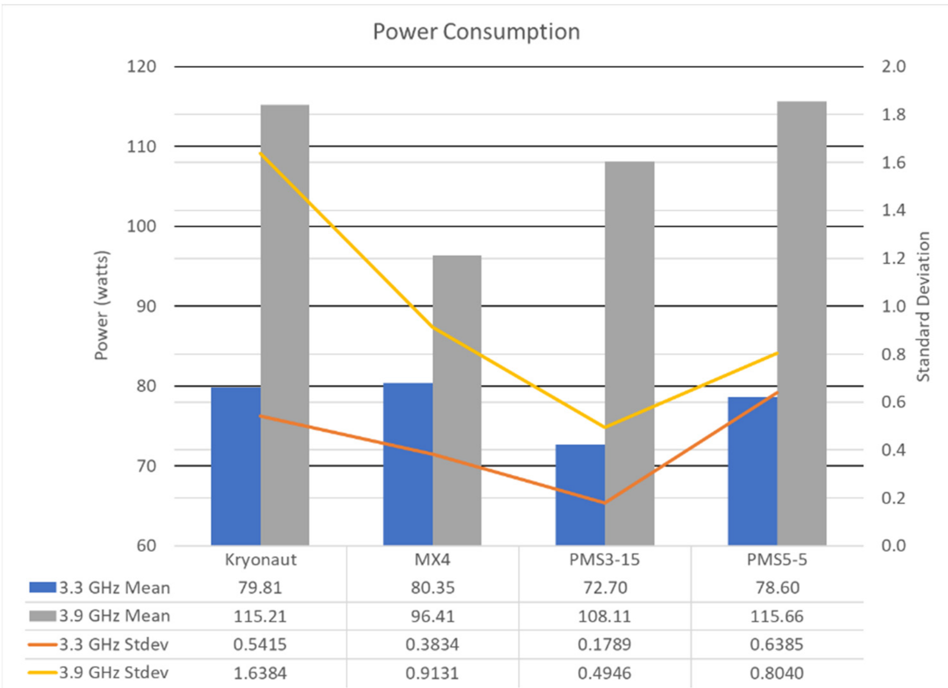

	Kryonaut	MX4	PMS3-15	PMS5-5
3.3 GHz Mean	79.81	80.35	72.70	78.60
3.9 GHz Mean	115.21	96.41	108.11	115.66
3.3 GHz Stdev	0.5415	0.3834	0.1789	0.6385
3.9 GHz Stdev	1.6384	0.9131	0.4946	0.8040

Figure 3. Average CPU Power Consumption.

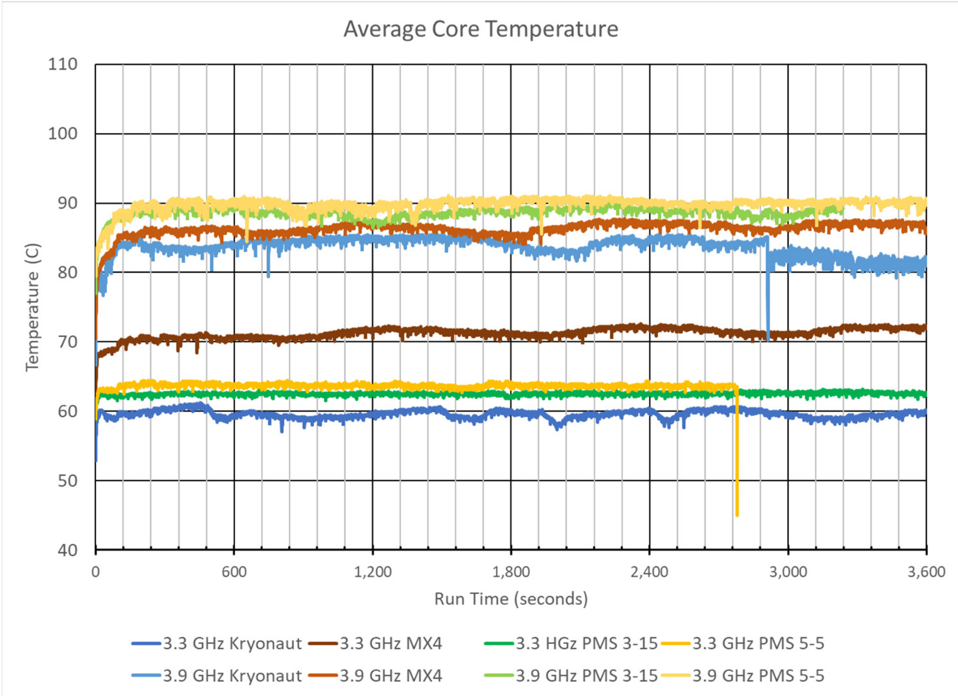

Figure 4. Average CPU core temperature.

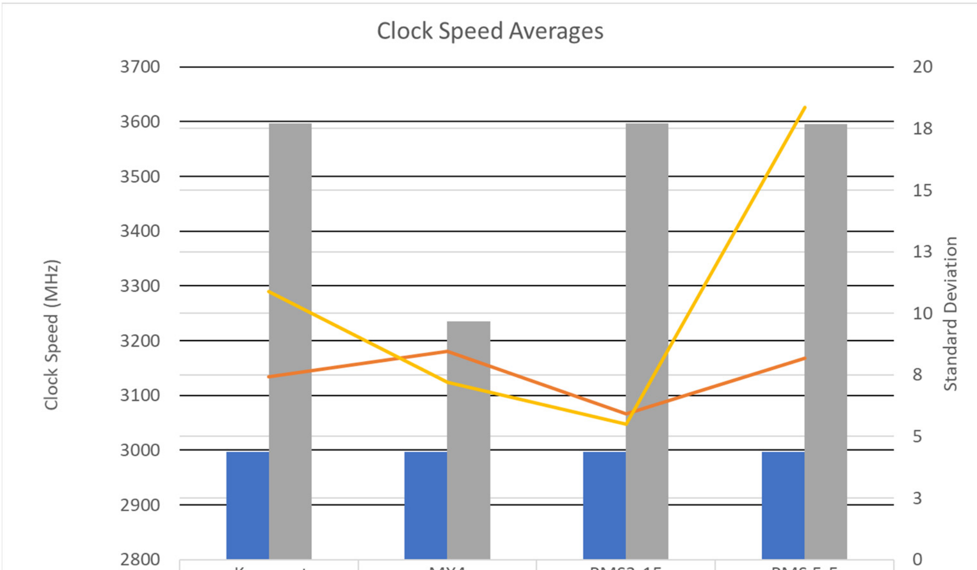

	Kryonaut	MX4	PMS3-15	PMS 5-5
3.3 GHz Mean	2,996.906	2,996.325	2,996.832	2,997.021
3.9 Ghz Mean	3,596.596	3,235.552	3,596.171	3,594.920
3.3 Ghz Stdev	7.4195	8.4616	5.9309	8.1871
3.9 GHz Stdev	10.8838	7.1953	5.5041	18.3575

Figure 5. Average CPU clock speed.

PMS silicone oil has been found to have a thermal conductivity of 0.152 W/mK. Various tested combinations of this oil and MWNT-OH and hBN have been accomplished, with the thermal-conductivity-result increases varying anywhere from 15% to 83%. The hydrogen bonding forms between the MWNTs-OH and the PMS silicone oil and creates a better path for the heat to travel on, thus increasing the thermal conductivity of the grease and the device performance.

A higher concentration of CNTs will cause the grease to become very dry and thick, while higher concentrations of hBN will result in liquid solutions. The data from these tests suggest a higher concentration of hBN to CNTs is necessary for a better performing grease.

Both Tables 1 and 2 show data averages for each core between the two testing speeds with an average for comparison to the three figures above. Clock speeds for each core should be within 1 MHz for stability and max performance. The significant variance between cores suggests an incorrect loading from BIOS or a CPU power flow error. Temperatures between cores can vary based on material composition and/or fabrication and thermal-compound application.

According to Table 1, the only test that had such a variance was MX4 in the overclock test. A majority of the cores have a drastic performance drop of 600 MHz. The data alone make it unclear what could have caused this issue.

Table 1. Clock-speed data.

Mean									
	3.3 GHz Testing					3.9 GHz Testing			
	Kryonaut	MX4	PMS3-15	PMS 5-5		Kryonaut	MX4	PMS3-15	PMS 5-5
Core #0	2996.968	2996.356	2996.820	2997.016	Core #0	3597.356	3595.251	3596.214	3598.422
Core #1	2996.927	2996.317	2996.860	2997.070	Core #1	3597.020	3595.251	3596.167	3597.253
Core #2	2996.886	2996.317	2996.820	2997.016	Core #2	3596.432	3593.069	3596.167	3572.338
Core #3	2996.886	2996.317	2996.820	2997.016	Core #3	3596.432	3595.251	3596.167	3597.201
Core #4	2996.886	2996.317	2996.820	2997.016	Core #4	3596.516	2996.116	3596.167	3597.175
Core #5	2996.886	2996.317	2996.820	2997.016	Core #5	3596.474	2996.116	3596.167	3597.201
Core #6	2996.886	2996.317	2996.901	2997.016	Core #6	3596.432	2996.116	3596.167	3597.851
Core #7	2996.886	2996.317	2996.820	2997.016	Core #7	3596.432	2996.116	3596.167	3597.318
Core #8	2996.969	2996.356	2996.820	2997.016	Core #8	3596.432	2996.116	3596.167	3597.201
Core #9	2996.886	2996.317	2996.820	2997.016	Core #9	3596.432	2996.116	3596.167	3597.240
Mean	2996.906	2996.325	2996.832	2997.021	Mean	3596.596	3235.552	3596.171	3594.920
Standard Deviation									
	3.3 GHz Testing					3.9 GHz Testing			
	Kryonaut	MX4	PMS3-15	PMS 5-5		Kryonaut	MX4	PMS3-15	PMS 5-5
Core #0	8.571	9.006	5.645	8.083	Core #0	18.769	6.295	6.581	21.081
Core #1	7.855	8.326	6.654	9.125	Core #1	16.091	6.295	5.384	12.880
Core #2	7.019	8.326	5.645	8.083	Core #2	9.002	19.466	5.384	65.369
Core #3	7.019	8.326	5.645	8.083	Core #3	9.002	6.295	5.384	10.680
Core #4	7.019	8.326	5.645	8.083	Core #4	10.290	5.601	5.384	11.516
Core #5	7.019	8.326	5.645	8.083	Core #5	9.678	5.601	5.384	10.680
Core #6	7.019	8.326	7.491	8.083	Core #6	9.002	5.601	5.384	17.283
Core #7	7.019	8.326	5.645	8.083	Core #7	9.002	5.601	5.384	12.316
Core #8	8.635	9.006	5.645	8.083	Core #8	9.002	5.601	5.384	10.553
Core #9	7.019	8.326	5.645	8.083	Core #9	9.002	5.601	5.384	11.216
Mean	7.419	8.462	5.931	8.187	Mean	10.884	7.195	5.504	18.358

Table 2. Temperature data.

Mean									
3.3 GHz Testing					3.9 GHz Testing				
	Kryonaut	MX4	PMS3-15	PMS5-5		Kryonaut	MX4	PMS3-15	PMS5-5
Core #0	52.9	59.6	57.1	57.3	Core #0	72.0	78.1	79.1	80.1
Core #1	60.7	74.5	64.1	63.3	Core #1	84.2	95.3	91.1	88.8
Core #2	67.2	79.1	68.9	71.4	Core #2	97.6	102.5	99.8	103.2
Core #3	62.8	77.8	64.2	65.3	Core #3	89.8	100.5	93.7	92.7
Core #4	53.3	65.9	57.0	58.1	Core #4	72.3	72.9	77.3	79.9
Core #5	56.2	60.1	60.4	62.2	Core #5	77.2	66.9	84.0	87.6
Core #6	61.6	75.6	63.0	64.1	Core #6	87.2	90.9	90.3	90.0
Core #7	60.1	74.4	63.3	62.8	Core #7	83.9	88.3	90.3	87.9
Core #8	65.9	79.3	68.3	70.9	Core #8	95.2	94.9	98.0	101.4
Core #9	55.6	66.6	59.1	61.7	Core #9	77.7	72.9	82.8	87.1
Mean	59.6	71.3	62.5	63.7	Mean	83.7	86.3	88.6	89.9
Standard Deviation									
3.3 GHz Testing					3.9 GHz Testing				
	Kryonaut	MX4	PMS3-15	PMS5-5		Kryonaut	MX4	PMS3-15	PMS5-5
Core #0	1.0	1.0	0.7	0.8	Core #0	3.2	1.7	1.2	1.7
Core #1	0.8	1.1	0.5	0.8	Core #1	3.9	1.7	1.1	1.8
Core #2	0.8	1.0	0.6	0.9	Core #2	1.6	1.6	1.4	1.2
Core #3	0.7	1.0	0.4	0.6	Core #3	1.2	1.3	1.4	1.1
Core #4	0.7	0.8	0.2	0.4	Core #4	2.8	1.0	0.8	1.0
Core #5	0.6	0.7	0.5	0.6	Core #5	2.7	0.9	0.7	0.9
Core #6	0.6	0.9	0.6	0.6	Core #6	1.4	1.3	1.2	1.5
Core #7	0.7	0.8	0.5	0.5	Core #7	1.9	1.3	0.9	1.3
Core #8	1.2	0.9	0.7	0.6	Core #8	1.8	1.3	1.3	1.3
Core #9	0.6	0.8	0.3	0.5	Core #9	1.1	1.0	0.6	0.9
Mean	0.8	0.9	0.5	0.6	Mean	2.2	1.3	1.1	1.3

In BIOS, many aspects of a PC can be controlled for customized performance, such as RAM speeds, fan control, CPU core control, and XMP (Extreme Memory Profile). Between tests, the computer is restarted to set the CPU core clock speeds in BIOS. Normally, other settings do not change between booting sequences, but this may not have been the case in this situation. An alternative hypothesis is Intel's automatic power control settings, which is a load control based on heat buildup. The other tests were performed normally and again showed that PMS3-15 provided a much more stable performance.

From Table 2, cores 0, 4, and 9 have lower temperatures than the rest of the cores. This suggests that either application of thermal compounds was consistent and/or the Prime95 runtime process was consistent. Although Kryonaut had the lowest temperatures of every compound, the stability of PMS3-15 indicates improved thermal transfer.

4. Conclusions

CNTs combined with hBN have significantly increased the silicone oil's thermal conductivity. CPU bench-testing data have shown an increase in thermal transfer and an increase in performance stability. The thermal stability of the modified grease reveals more than two times enhancement for the control. In addition, the manufactured grease was found to have the same performance and improved stability compared to the commercial thermal grease for both clock speeds and temperature. However, PMS3-15 had the same clock speeds, maintained within 5 °C, and improved stability by 100% when is compared by the other popular thermal grease Kryonaut.

Author Contributions: T.G.: writing—original draft writing, reviewing, and editing; G.C.: writing—original draft writing, reviewing, and editing; C.B.: concept, investigation, supervision, writing—reviewing, and editing; D.L.: writing—original draft writing, reviewing, and editing; H.H.: writing—reviewing, and editing; H.Y.: concept, investigation supervision, writing—reviewing, and editing. All authors have read and agreed to the published version of the manuscript.

Funding: This research was funded by AFWERX, grant number FA86921P0028.

Data Availability Statement: Not applicable.

Acknowledgments: The authors would like to thank Mingyang Mao for their help with the preparation of some samples.

Conflicts of Interest: The authors declare no conflict of interest.

References

1. Siricharoenpanich, A.; Wiriyasart, S.; Naphon, P. Study on the thermal dissipation performance of GPU cooling system with nanofluid as coolant. *Case Stud. Therm. Eng.* **2021**, *25*, 100904. [CrossRef]
2. Bahiraei, M.; Heshmatian, S. Electronics cooling with nanofluids: A critical review. *Energy Convers. Manag.* **2018**, *172*, 438–456. [CrossRef]
3. Naphon, P.; Wiriyasart, S.; Wongwises, S. Thermal cooling enhancement techniques for electronic components. *Int. Commun. Heat Mass Transf.* **2015**, *61*, 140–145. [CrossRef]
4. Ma, K.-Q.; Liu, J. Heat-driven liquid metal cooling device for the thermal management of a computer chip. *J. Phys. D Appl. Phys.* **2007**, *40*, 4722. [CrossRef]
5. Li, H.-Y.; Chao, S.-M.; Tsai, G.-L. Thermal performance measurement of heat sinks with confined impinging jet by infrared thermography. *Int. J. Heat Mass Transf.* **2005**, *48*, 5386–5394. [CrossRef]
6. Naphon, P.; Wiriyasart, S. Liquid cooling in the mini-rectangular fin heat sink with and without thermoelectric for CPU. *Int. Commun. Heat Mass Transf.* **2009**, *36*, 166–171. [CrossRef]
7. Stephan, K.; Laesecke, A. The thermal conductivity of fluid air. *J. Phys. Chem. Ref. Data* **1985**, *14*, 227–234. [CrossRef]
8. Shishkin, R.A. Investigation of Thermal Greases with Hybrid Fillers and Its Operational Bench Test. *J. Electron. Mater.* **2022**, *51*, 1189–1201. [CrossRef]
9. Christensen, G.; Younes, H.; Hong, H.; Peterson, G. Alignment of carbon nanotubes comprising magnetically sensitive metal oxides by nonionic chemical surfactants. *J. Nanofluids* **2013**, *2*, 25–28. [CrossRef]
10. Wu, S.-W.; Chang, T.-C.; Lin, Y.-H.; Chen, H.-F.; Fuh, Y.-K. Fabrication of copper powder hybrid supported fillers with interconnected 1D/2D/3D nanostructures for enhanced thermal interface materials properties. *Int. J. Adv. Manuf. Technol.* **2022**, *121*, 3453–3462. [CrossRef]
11. Li, J.; Zhang, Y.; Liang, T.; Bai, X.; Pang, Y.; Zeng, X.; Hu, Q.; Tu, W.; Ye, Z.; Du, G. Thermal interface materials with both high through-plane thermal conductivity and excellent elastic compliance. *Chem. Mater.* **2021**, *33*, 8926–8937. [CrossRef]
12. Chen, H.; Wei, H.; Chen, M.; Meng, F.; Li, H.; Li, Q. Enhancing the effectiveness of silicone thermal grease by the addition of functionalized carbon nanotubes. *Appl. Surf. Sci.* **2013**, *283*, 525–531. [CrossRef]
13. Hansson, J.; Nilsson, T.M.J.; Ye, L.; Liu, J. Novel nanostructured thermal interface materials: A review. *Int. Mater. Rev.* **2018**, *63*, 22–45. [CrossRef]
14. Ge, X.; Chen, Y.; Liu, W.; Zhang, G.; Li, X.; Ge, J.; Li, C. Liquid cooling system for battery modules with boron nitride based thermal conductivity silicone grease. *RSC Adv.* **2022**, *12*, 4311–4321. [CrossRef]
15. Christensen, G.; Younes, H.; Hong, G.; Lou, D.; Hong, H.; Widener, C.; Bailey, C.; Hrabe, R. Hydrogen bonding enhanced thermally conductive carbon nano grease. *Synth. Met.* **2020**, *259*, 116213. [CrossRef]
16. Christensen, G.; Grablander, T.; Bailey, C.; Lou, D.; Hong, H. Increasing Engine Efficiency with Friction Reducing-Oil Additives. In Proceedings of the TechConnect Briefs, Washington, DC, USA, 18 October 2021; pp. 267–270.
17. Ren, P.-G.; Si, X.-H.; Sun, Z.-F.; Ren, F.; Pei, L.; Hou, S.-Y. Synergistic effect of BN and MWCNT hybrid fillers on thermal conductivity and thermal stability of ultra-high-molecular-weight polyethylene composites with a segregated structure. *J. Polym. Res.* **2016**, *23*, 21. [CrossRef]
18. Yu, W.; Xie, H.; Yin, L.; Zhao, J.; Xia, L.; Chen, L. Exceptionally high thermal conductivity of thermal grease: Synergistic effects of graphene and alumina. *Int. J. Therm. Sci.* **2015**, *91*, 76–82. [CrossRef]

19. Chen, C.; He, Y.; Liu, C.; Xie, H.; Yu, W. Comprehensive excellent performance for silicone-based thermal interface materials through the synergistic effect between graphene and spherical alumina. *J. Mater. Sci. Mater. Electron.* **2020**, *31*, 4642–4649. [CrossRef]
20. Liang, W.; Ge, X.; Ge, J.; Li, T.; Zhao, T.; Chen, X.; Zhang, M.; Ji, J.; Pang, X.; Liu, R. Three-Dimensional Heterostructured Reduced Graphene Oxide-Hexagonal Boron Nitride-Stacking Material for Silicone Thermal Grease with Enhanced Thermally Conductive Properties. *Nanomaterials* **2019**, *9*, 938. [CrossRef]
21. Younes, H.; Christensen, G.; Horton, M.; Al Ghaferi, A.; Hong, H.; Qiang, Y. TC study of manufacturable nano grease: Evidence of 3D network structure. *Nanomanuf. Metrol.* **2018**, *1*, 148–155. [CrossRef]
22. Younes, H.; Lou, D.; Hong, H.; Chen, H.; Liu, H.; Qiang, Y. Manufacturable Novel Nanogrease with Superb Physical Properties. *Nanomanufacturing Metrol.* **2021**, *4*, 289–297. [CrossRef]
23. Christensen, G.; Yang, J.; Lou, D.; Hong, G.; Hong, H.; Tolle, C.; Widener, C.; Bailey, C.; Hrabe, R.; Younes, H. Carbon nanotubes grease with high electrical conductivity. *Synth. Met.* **2020**, *268*, 116496. [CrossRef]
24. Nazari, M.; Karami, M.; Ashouri, M. Comparing the thermal performance of water, Ethylene Glycol, Alumina and CNT nanofluids in CPU cooling: Experimental study. *Exp. Therm. Fluid Sci.* **2014**, *57*, 371–377. [CrossRef]
25. Ebrahimi, S.; Sabbaghzadeh, J.; Lajevardi, M.; Hadi, I. Cooling performance of a microchannel heat sink with nanofluids containing cylindrical nanoparticles (carbon nanotubes). *Heat Mass Transf.* **2010**, *46*, 549–553. [CrossRef]
26. Guo, W.; Li, G.; Zheng, Y.; Dong, C. Numerical study of nanofluids thermal and hydraulic characteristics considering Brownian motion effect in micro fin heat sink. *J. Mol. Liq.* **2018**, *264*, 38–47. [CrossRef]
27. Lou, D.; Grablander, T.; Mao, M.; Hong, H.; Peterson, G. Improved thermal conductivity of PEG-based fluids using hydrogen bonding and long chain of nanoparticle. *J. Nanoparticle Res.* **2021**, *23*, 98. [CrossRef]